

# A study on Vertical Structure of Marine Atmospheric Boundary Layer over Pacific Ocean

R.Madhuri<sup>1,2</sup>, R.Suneetha<sup>3</sup> and T.Subba Rao<sup>1</sup>

<sup>1</sup>Dept. of Physics, Sri Krishnadevaraya University, Anantapuram, India

<sup>2</sup>SML Government Degree College, Yemmiganur, Andhra Pradesh, India

<sup>3</sup>Silver Jubilee Government Degree College, Kunrool, Andhra Pradesh, India

## Abstract:

We are carrying out research at Palau Islands focusing on the Pacific Area Long-term Atmospheric observation for Understanding of climate change (PALAU) project to understand the mechanism of cloud-precipitation processes, land-atmosphere and air-sea interactions over the warm water pool, focusing on seasonal and intra-seasonal variations. We installed several ground based remote sensors at Peleliu and Aimeliik experimental sites in the Palau. For the present study, Wind Profiler Radar (WPR) is utilized for understanding of the marine boundary layer (MABL) evolution, diurnal and seasonal variation of precipitating cloud systems associated with easterly and westerly monsoon. In the present study, long-term (four year) observations of the marine boundary layer height using wind profiler radar are utilized to estimate ventilation coefficient, a critical parameter in determining air pollution concentration near the surface which signifies the ability for natural ventilation of air over Palau in Tropical Western Pacific Ocean during the period from April 2003 to March 2007. In addition, MABL observations revealed that well-distinguishable features during westerly, easterly and transition period.

Key Words: Marine atmospheric boundary layer (MABL) ; Wind profiling radar;

## 1. Introduction:

The dynamics of the Marine Boundary Layer (MABL) is a complex problem involving oceanic and atmospheric processes as well as interactions at the air-sea interface. Progress towards improving the theoretical understanding of the MABL has been hampered not only by the difficulty of modeling these often nonlinear processes and interactions but also by the difficulty of carrying out experimental programs at sea. Furthermore, the role of intermittent and directional processes is now beginning to be addressed, and a better understanding of these processes is viewed as critical in determining air-sea fluxes of momentum, heat, and moisture.

Due to lack of direct measurements of boundary layer height and of suitable measurements that could be used to estimate it <sup>1</sup>, the boundary layer height is less common in the climatological literature. This problem may be partially remedied through analysis of new data sources like observations by radio occultation measurements from global navigational satellite systems <sup>2,3</sup>, aerosol observations from satellites <sup>4</sup>, Lidar<sup>5</sup> and Sodar<sup>6</sup>. Other types of observations, including Wind-profiling and boundary layer Radar<sup>7,8</sup> and Ceilometer<sup>9</sup> have been used to estimate boundary layer height. During the past two decades Doppler wind radar profilers (WPR) that operate near 1 GHz have been used in boundary layer dynamics and precipitation research. The advantage of this WPR is to measure directly the vertical wind component within a convective environment. Hence, WPR has been used extensively used in numerous

field campaigns during the past couple of decades<sup>10</sup>. WPR observations yield time height cross-sections of equivalent reflectivity, Doppler velocity and spectral width that illustrate the evolution of boundary layer and precipitating clouds systems.

## 2. Location, Data Sources and Measurements Techniques

Institute of Observational Research for Global Change has been conducted the observational project PALAU (Pacific Area Long-term Atmospheric observation for the Understanding of climate change ) over Peleliu Island (7.05°N, 134.27 °E) and Aimeliik state of Babeldaob Island (7.45° N, 134.47° E) of Republic of Palau (Fig. 1). National weather service (NWS) which is confided by National Oceanic and Atmospheric Administration (NOAA) is located at Koror (7.33°N, 134.48°E) the capital of Palau. At Aimeliik Observatory, Wind profiler radar (WPR) with Radio acoustic sounding system, Impact type disdrometer, Micro Rain Radar, Ceilometer, Microwave Radiometer and Automatic Weather Station (AWS), Ceilometer are installed and continuous gathering data. Aimeliik is located in the high island of Babeldaob [in the Palau (508 Sq. km) archipelago], which is one of the largest islands in the western Pacific Ocean. Babeldaob Island is partly elevated limestone and partly volcanic. The vegetation in this island varies from the mangrove swamps of the coast, with trees often from 10–16 meters high; to the savannah type grasslands of the near interior which support palms and pandanus, and the densely forested valleys further inland.

For the present study, four years data from 01 April 2003 to 31 March 2007 has been utilized. The upper range of these profiles typically reaches 500–1000 m above ground. During the observational period, no availability of the data for several days was mainly due to external power failure, system maintenance, and severe weather hazards. For detailed WPR description, data collection and operation strategy, refer to Reddy et al.<sup>13</sup>. Upper air sounding is carried out by Koror National Weather Service (NWS) which is located about 10 km south of Aimeliik observatory. Balloons are launched twice a day i.e. around 0000 and 1200 UTC. Additional 2 or 3 balloons released by the NWS during intensive observational periods.

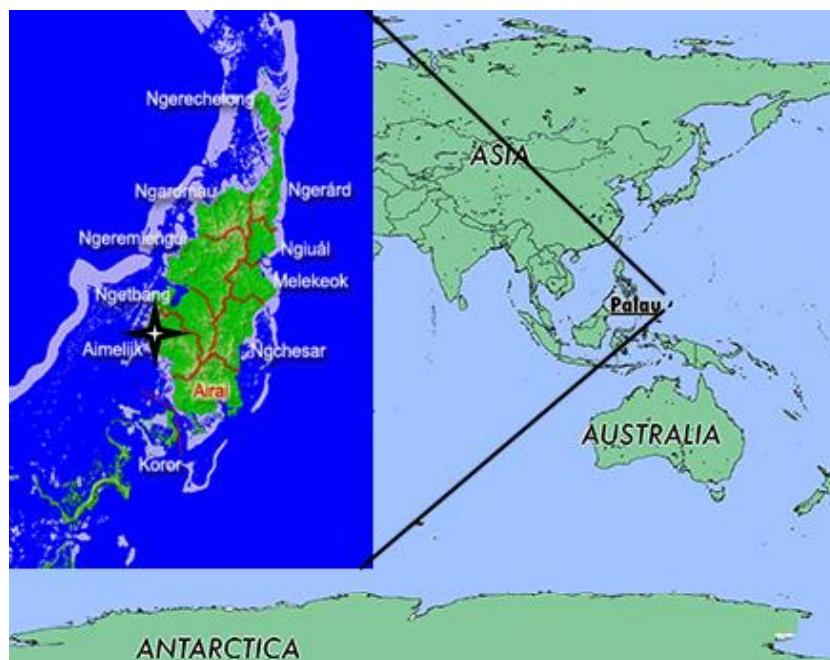


*Fig. 1: Map showing location of Aimeliik Observatory over Palau Islands, in Pacific Ocean*

### 3. Evolution of MABL height:

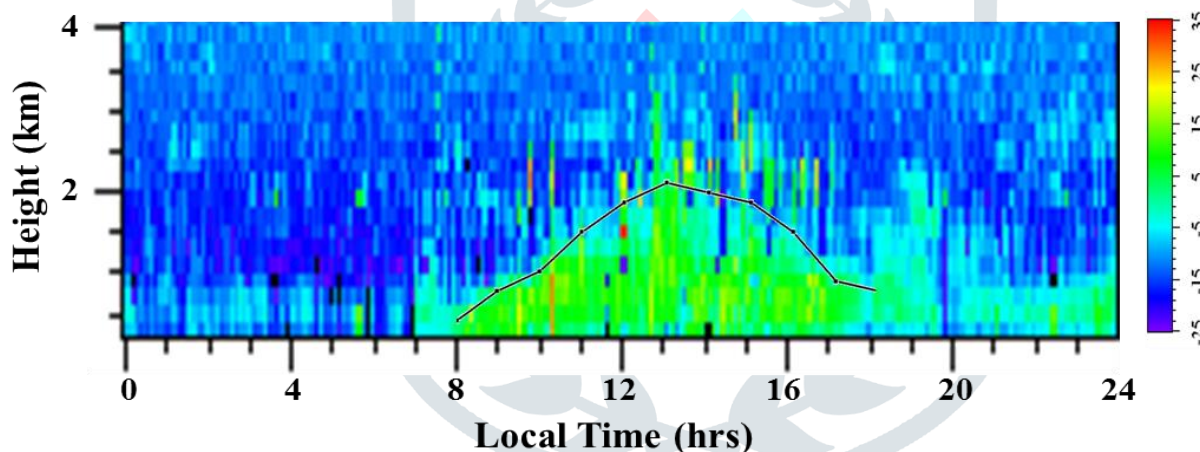


*Fig. 2: Time height profile of radar reflectivity during 02<sup>nd</sup> July 2003 over Palau. The solid line represents the hourly averaged MABL height derived from radar reflectivity*

For the present study, we analyzed four year variations in the MABL height over Palau using wind profiler radar and Radiosonde data. Wind profiler radar offers the unique ability to directly measure vertical motion profiles through precipitating and non-precipitating cloud systems (Reddy et al. 2002). So wind profiler radars can be used to determine the MABL height during both precipitating and non-precipitating events. As an example, time height profile of radar reflectivity during 02<sup>nd</sup> July 2003 (non-precipitating event) is shown in Fig. 2. The solid line in figure 3 represents the hourly averaged MABL height derived from radar reflectivity during 0800 to 1800 local time (LT) on the same day. When the amount of incoming solar radiation increases in the morning hours, then MABL height also increases and reaches its maximum

in the afternoon. When the solar elevation decreases, the available energy is small, so the thermally-driven turbulence decays and vertical mixing decreases and hence the MABL height decreases.

### Comparison of MABL height derived from WPR and Radiosonde Measurements:

Maximum mixing depth (MMD) derived from individual radiosonde profile are compared with the mean MABL height derived from WPR measurement. 30 minutes average of MABL height measured between 0000& 0030 GMT and 1200& 1230 GMT using WPR during non-rainy days are compared with the radiosonde profile during respective days. The scatter plot of the boundary layer depths derived from the wind profiler and radiosonde (Fig. 4) show a reasonably good agreement between the two methods. The observed discrepancies are expected because, radiosonde provides a “snapshot” of the state of the atmosphere as they ascend. Therefore, the mixing height determined from radiosonde data represents a point measurement in space and time. Hence, WPR can be used to monitor the boundary layer height in a continuous fashion as radiosonde data is not available continuously.

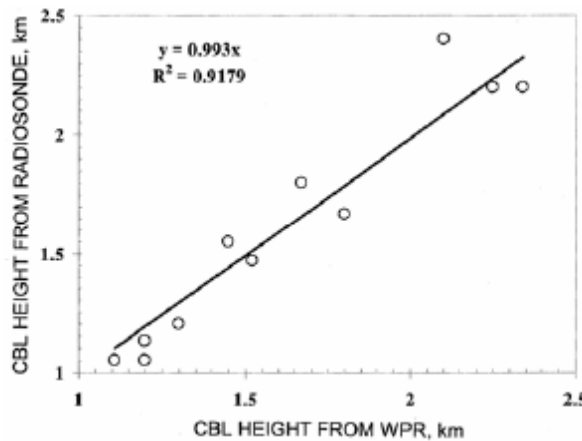


**Fig. 3 : Scatter plot of convective boundary layer heights estimated from the wind profiler and radiosonde observations**

### 3.2 Temporal Variation of MABL height and VC:

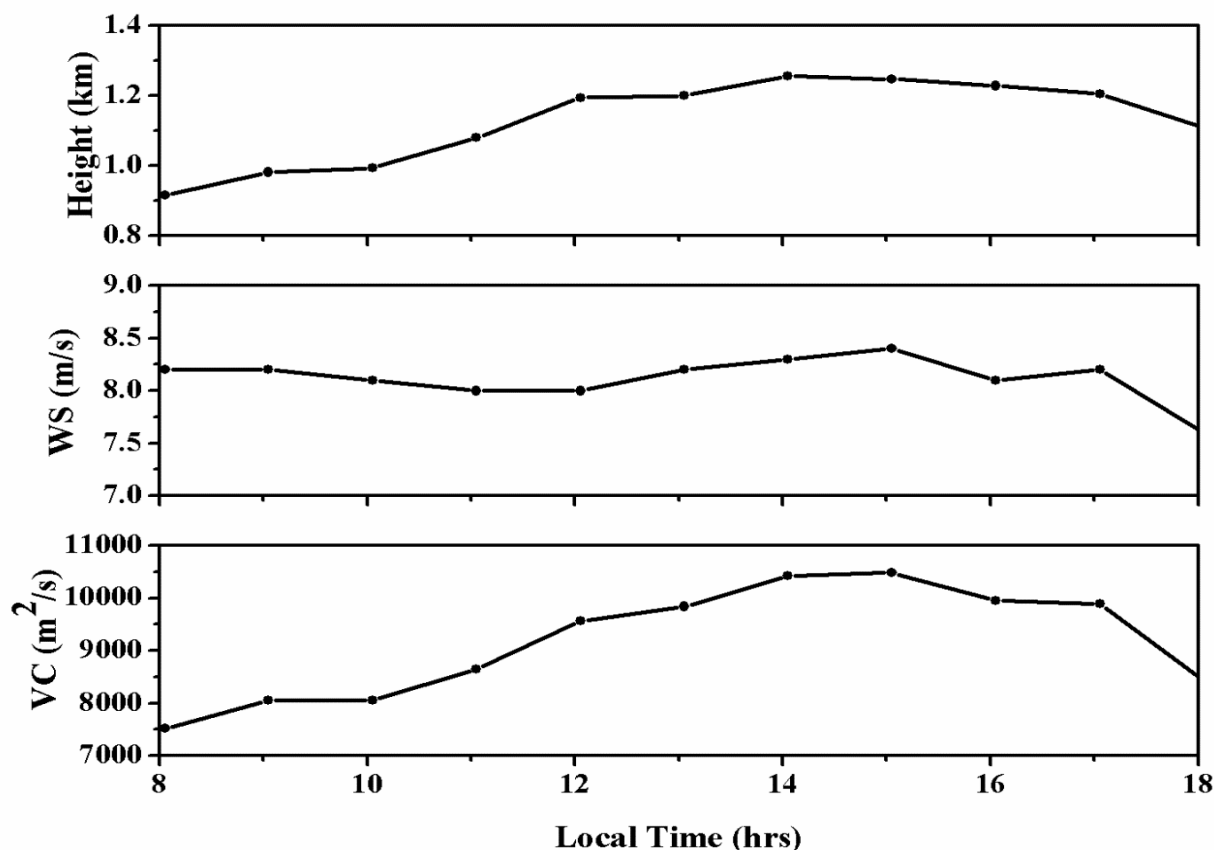


**Fig. 4: Diurnal evolution of MABL height, mean wind speed with in MABL and ventilation coefficient during 0600 to 1800 local time on 15<sup>th</sup> January, 2004.**

Diurnal evolution of mean MABL height during 0800 to 1800 LT is shown in Figure 4a. It is observed that the MABL depth is low during morning hours, increases gradually with time after sunrise and reaches a higher value at noon hours and starts decreasing in the evening. This is the general behaviour of daytime boundary layer during clear air days. The increased MABL height after sunrise may be connected to the start of the sea breeze from the surrounding marine atmosphere and hence turbulence becomes stronger and the MABL height grows steadily after sun rise.

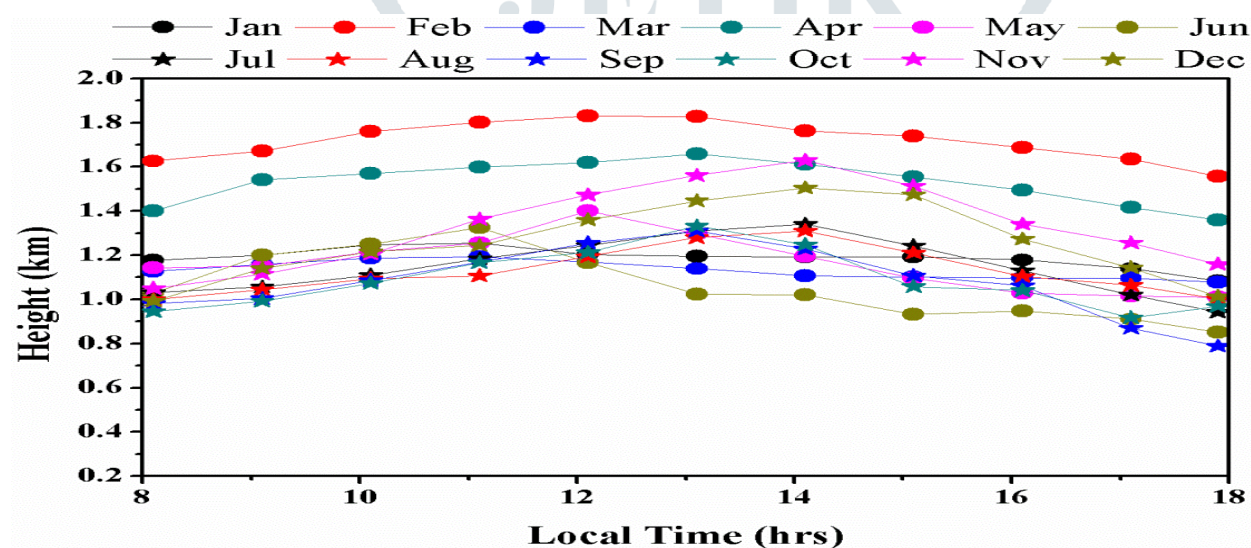
The evolution of the daytime boundary layer can influence the aerosol particle concentration and size distribution at the ground level. In the early morning hours when the MABL depth is low, there can be accumulation of pollutants near the surface. After sunrise, the boundary layer starts evolving with time. Hence the pollutants trapped in the ground-based stable layers during the previous night are dispersed and transported to other regions of the lower atmosphere by turbulent mixing. During evening hours, the pollutants emitted can be constrained at the lower heights in the boundary layer and can remain until early morning hours due to the formation of nocturnal stable boundary layer. Thus the diurnal behaviour of the boundary layer plays an important role in aerosol particle concentration at the ground level. This is further evident from the variation of VC. Figure 4b and 4c represents the temporal variation of average wind speed

within the boundary layer and ventilation coefficient respectively. The diurnal variation of VC shows low values during early morning hours, it gradually increases and reaches maximum value during the noon hours and decreases in the evening. This indicates the high dispersive capacity of MABL during afternoon hours.

### 3.3 Monthly and Seasonal Variations of VC:

Fig. 5 shows the monthly averaged diurnal variation of MABL height during 2003 to 2007. The months of February, April and November show the longest and highest MABL heights whereas the months June, August and September the lowest MABL height. The higher MABL height during April and November is due to higher sunshine hours. However the higher MABL height during February is due to availability of less number of data during February. For this reason, we will not consider the MABL height in February as maximum in the calculation of ventilation coefficient. MABL heights are lowest during June, August and September which corresponds to the lowest average sunshine hours.

*Fig. 5: Monthly mean of daily hourly averaged MABL heights over Palau.*



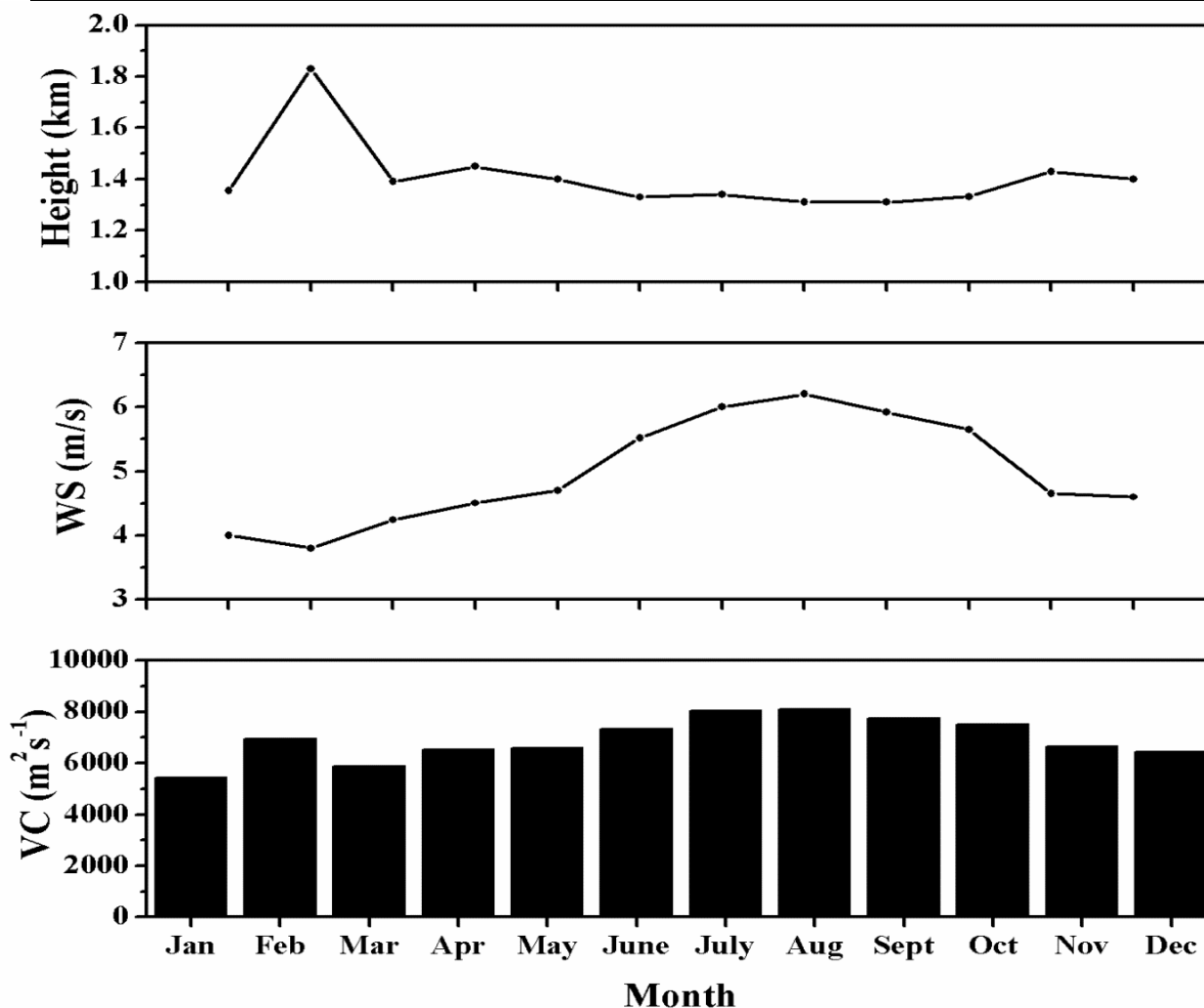


**Fig. 6: Monthly variation of mean noon-time MABL height and VC over Palau during April, 2003 to March, 2007**

To study the monthly variation of VC, monthly mean of maximum MABL height for each day and the corresponding wind speed within the boundary layer are given in figure 6a and b for the year 2004. This is used to estimate the monthly average of VC (Figure 6c). It is apparent that VC has the highest value during August ( $\sim 8122 \text{ m}^2\text{s}^{-1}$ ) and lowest during January ( $5424 \text{ m}^2\text{s}^{-1}$ ). The MABL height is high during April and this reaches an average value of  $\sim 1.45 \text{ km}$ , whereas lower values are observed in September ( $\sim 1.3 \text{ km}$ ). During the other months the MABL height varies in the range  $\sim 1.3$  to  $1.5 \text{ km}$ . Maximum wind speed is observed during June, July and August. It can be seen that the variation of VC during the period November to April is influenced both by the MABL height and wind speed within the MABL, whereas during May to October, it closely follows the same type of variation as that of the wind speed. Note that the MABL height does not vary much from July to November. It can be noted from Figure 6 that the annual variation of MABL height is not as drastic as that of wind speed, and it is the larger increase in wind speed rather than MABL height that results in high VC during the monsoon months.

**Table.1:** Seasonal variation of MABL height and VC over Palau during April 2003 to March 2007.

Season/Climate	Months	Mean noon time MBL height (km)	Ventilation Coefficient ( $\text{m}^2\text{s}^{-1}$ )
Easterly monsoon	Late December to April	$1.28 \pm 0.26$	5670
Easterly to Westerly monsoon Transition	May and June	$1.11 \pm 0.17$	5120
Westerly monsoon	July to October	$1.19 \pm 0.21$	7020
Westerly to Easterly monsoon Transition	November to Early December	$0.97 \pm 0.16$	6230

To study the Seasonal variation of VC, the data is divided into four groups (Table 2) corresponding to Easterly (late December to April), Easterly to Westerly transition (May and June), Westerly (July to October) and Westerly to Easterly transition (November and Early December) periods. The average values of VC and mean noon time MABL height during April 2003 to March 2007 is shown in Table. 2. It is observed that VC is high during Westerly monsoon period ( $7020 \text{ m}^2\text{sec}^{-1}$ ) and low during Easterly to Westerly transition period ( $5120 \text{ m}^2\text{sec}^{-1}$ ). During Easterly monsoon period VC is  $5670 \text{ m}^2\text{sec}^{-1}$ , whereas during Westerly to Easterly transition VC is found to be  $6230 \text{ m}^2\text{sec}^{-1}$ . The high value of VC during Westerly monsoon period is due to high wind speed. Along with the high value of VC, washout processes by precipitation can result in a cleaner environment. However, low values in wind speed results in low values of VC during Westerly to Easterly transition period. This may be attributed to the increase of anthropogenic aerosol loading during Westerly to Easterly transition period which has profound effects on the climate change over this region (Intergovernmental Panel on Climate Change (IPCC) report, 2001). Ashrafiet al. (2009) estimated VC for Tehran region (Iran) and found that the VC values for spring and summer were higher than those for fall and winter. At Fort Simpson, Northwest Territories region, Yap (1974) found winter VC extremely low on most days due to low mixing depths frequently coupled with light winds through mixing layer. However in the present study, we reported low values in VC during transition period, moderate VC during Easterly and high VC during Westerly monsoon period.

#### 4. Evolution of MABL structures during easterly and westerly monsoon:

The vertical structure of atmospheric variables in the marine atmospheric boundary layer (MABL) plays an important role in the development of clouds at the top of the MABL in the initiation and maintenance of deep convection. An important parameter of the MABL is the MABL height that is controlled by surface forcing and entrainment at the MABL top as well as by advection. In recent years,



considerable progress has been made in the development, improvement, and application of active remote sensing systems such as Wind profiler radar for boundary layer research. Wind profiler offers the unique ability to directly measure vertical motion profiles through precipitating and non-precipitating cloud systems. Also, the wind profiler reflectivity provides a detailed record of the evolution of MABL throughout the day.

We adopted similar scheme proposed by Grimsdell and Angevine (1998) with a modification (added another category of the MABL evolution). In the present study, MABL evolution during precipitation is included to understand the influence of rain. We established that the following conditions had to be met for their inclusion in the MABL characterization under precipitating condition.

- (a) The reflectivity pattern shows growth of the MABL during the morning transition that indicated the presence and growth of boundary layer thermals.
- (b) During the afternoon, a discernible and coherent pattern should be seen in the reflectivity figure. The spectral width shows a similar pattern, indicating that the reflectivity is related to turbulent activity within the MABL.

The three categories were named descent, ascent and inversion layer (IL), based on the behavior of the profiler reflectivity in each category. The defining characteristics of the categories are as follows.

**Descent** — the reflectivity pattern shows growth of the MABL during the morning transition that indicated the presence and growth of boundary layer thermals. The reflectivity is strong throughout the MABL depth during the morning transition hours, with correspondingly large spectral width (not shown here), implying the presence of strong convection. From late afternoon to evening (i.e. in the evening transition hours – between 1600 and 1800 hrs LT), the maximum height reached by the strong reflectivity steadily decreased, while the signal strength remained constant and the spectral width remained small.

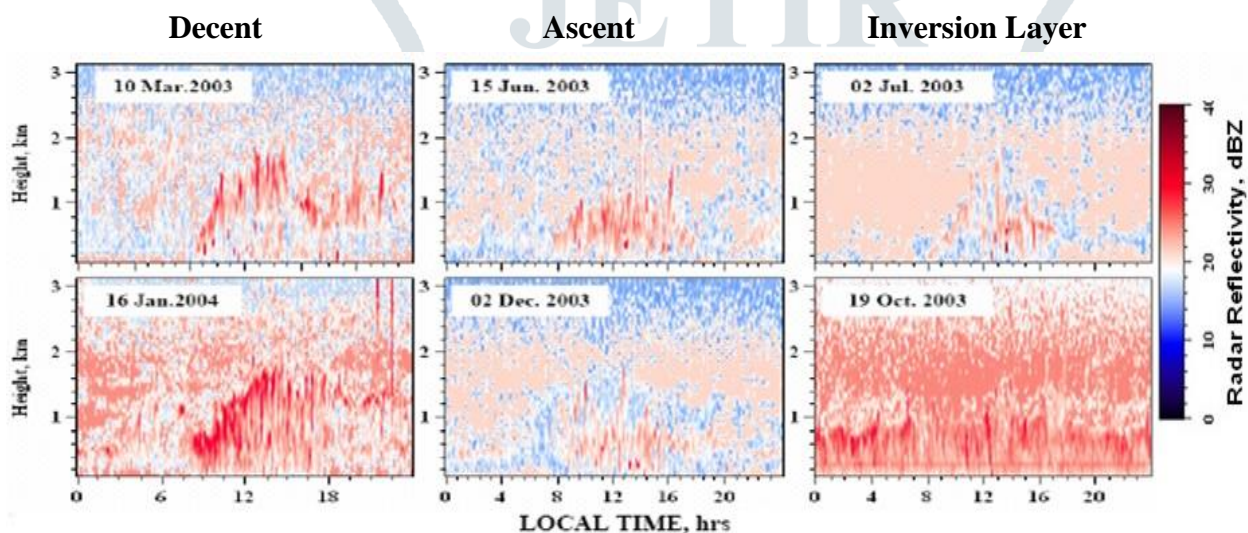
**Ascent** — during the morning, the reflectivity pattern shows MABL growth similar to that on the descent days. Moreover, MABL is continuously ascended after midday also. During the evening transition hours, mostly MABL will be ascended or disappeared.

**Inversion layer (IL)** — WPR reflectivity pattern shows MABL evolution similar to the descent days but throughout the day persistence of an inversion layer (mainly due to subsidence) between 1.5 and 3.5 km with strong reflectivity and also existence of the nocturnal multiple elevated layers (a few days in the daytime also).

WPR observational results depicted in Figure 7 shows that many variations in the evolution of MABL during the morning, afternoon and early evening, in contrast with the consistency seen during the nighttime. The definition of the three categories and the assignment of particular days to those categories based on two-dimensional patterns were necessarily subjective. Although it may be possible to describe these patterns with a small number of objective parameters, we did not do so; as such pattern recognition is a notoriously difficult problem.

Figure 7 [middle two panels] shows the evolution of MABL on ascent days during the westerly monsoon period. On these days, a shallow MABL confined to 1 km is observed most of the days. It is well known that during the westerly monsoon, boundary layer will be rich in moisture. So, most of the radiation from the surface will be utilized for the evaporation processes, which results in a shallow MABL. Enhanced soil moisture probably contributes to increase in the latent heat fluxes and thus decreasing the surface sensible flux locally and suppress the MABL growth, as compared to the deeper MABL that develops with reduced soil moisture level on pre-monsoon days. One more cause for the shallow MABL during the westerly monsoon days may be the increased upper level clouds that can reduce the incoming solar radiation.

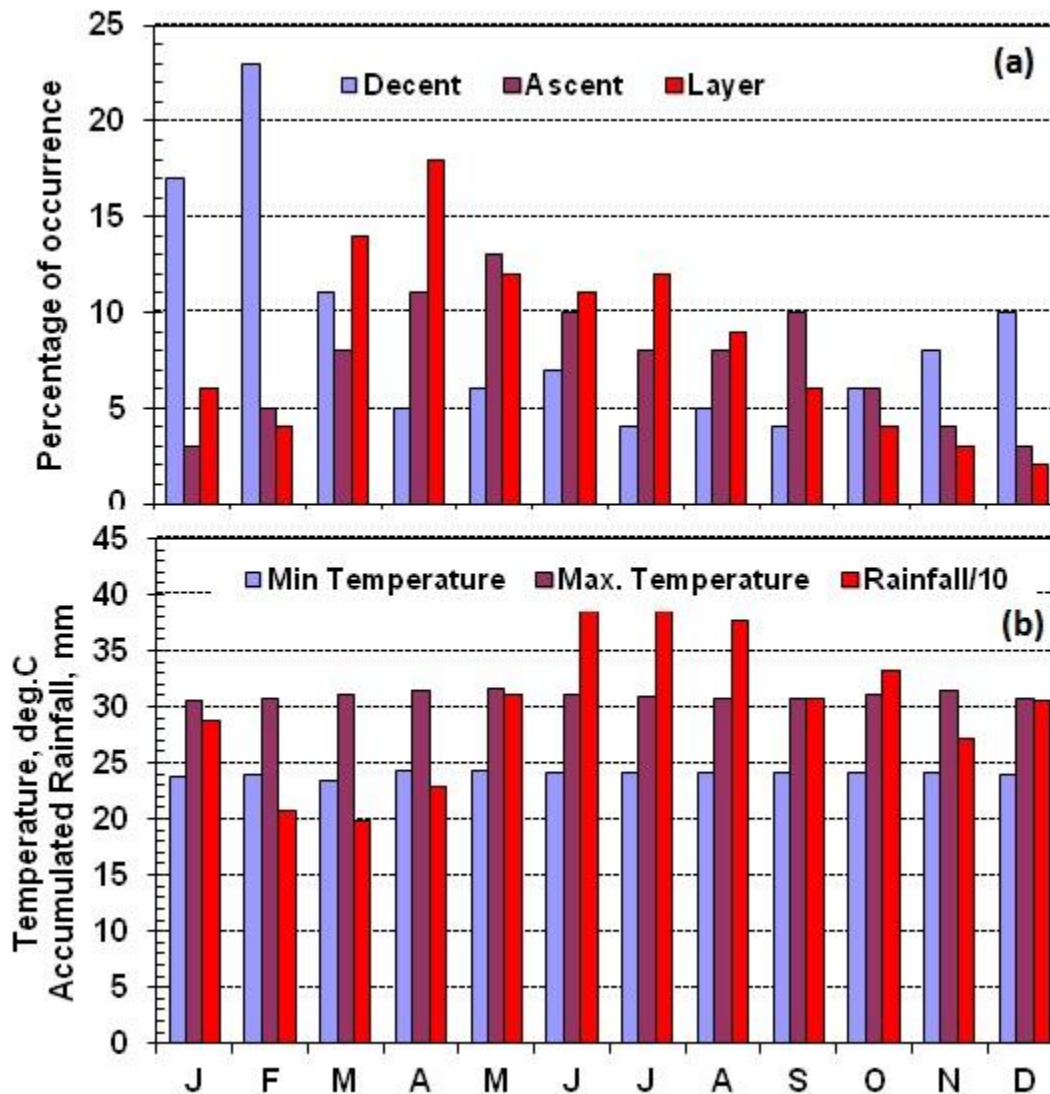
In moist conditions, more energy is partitioned into latent heat flux, leading to weaker convection. This effect is consistent with the formation of a weak capping inversion that was present during transition periods, usually its occurrence is maximum in Westerly monsoon period.



**Fig. 7: Time-height cross section of the Aimeliik wind profiler (vertical beam) range-corrected reflectivity (SNR) during clear-air convection days during different seasons.[Left two panels for descent type, middle two panels for ascent type and right two panels for inversion layer (IL) type].**

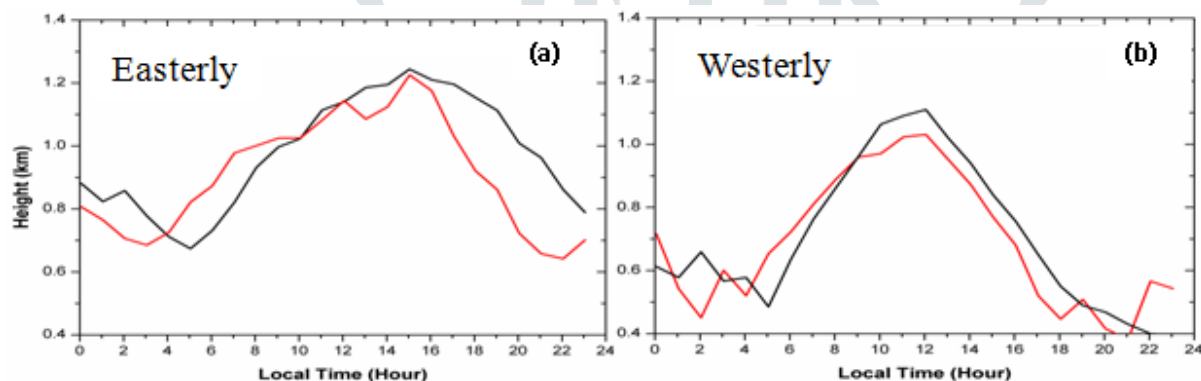
Figure 8 (a) show that the different daytime MABL structure has been found to exhibit considerable vertical variability during different seasons; a phenomenon attributed to the underlying topography and varied land surface-atmosphere interactions. Information from the surface weather maps (issued by Japan Meteorological Agency), Disdrometer, and Automatic weather station [figures are not shown here] data are examined to see whether there are any differences in the measured variables that could explain the observed differences in reflectivity between the three categories. Difference in temperature and humidity affects energy partitioning within MABL. In moist conditions, more energy is partitioned into latent heat flux,

leading to convection. This effect is consistent with the formation of a capping inversion that was present in the descent case; usually its occurrence is maximum in westerly monsoon period [Figure 8]. It is also a fact that the average MABL depth of descent days was low [max. occurrence in monsoon (average MABL height ~1.4 km)]. Occurrence of IL type MABL (average MABL depth ~ 2.6 km) evolution is maximum during winter, which could be due to the presence of early morning dew/fog that reduces the total available buoyant energy for the boundary layer and/or advection of warmer air from the Ocean through north-easterly/easterly wind over Aimeliik valley. During the month of January and February occurrence of Decent type MABL evolution is more pronounced due to less surface temperatures. The striking feature in the Ascent type is that the MABL (average MABL depth ~ 1.38) is continuously growing after 1200 hrs LT also. The Disdrometer and AWS precipitation measurements and minimum/maximum temperatures are shown in Figure 8(b). The deepening of the MABL is observed in the late afternoon in the Ascent type, whereas it is observed exactly at the midday for the descent type during dry convection days.



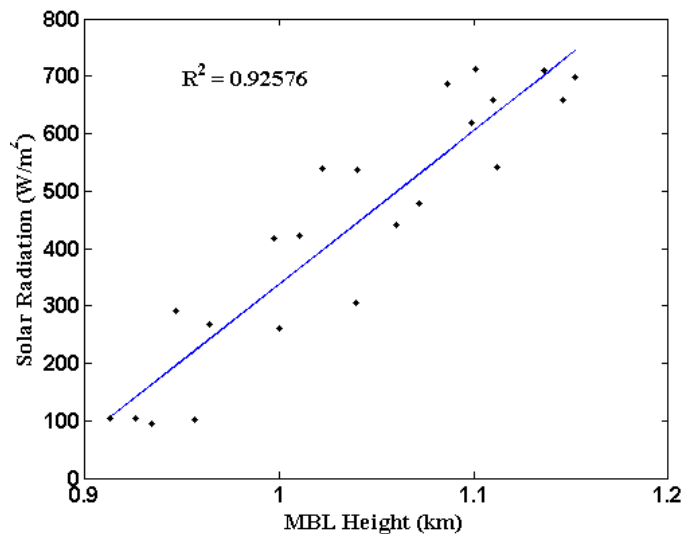
**Fig. 8. Evolution of monthly occurrence of Descent, Ascent and Inversion Layer type marine boundary layer structures observed during passage of precipitating clouds over Palau from April 2003 to March 2007.**

Figure 9(a) shows the evolution of MABL during easterly monsoon period. On these days, MABL developed at morning 0600 hrs and afterwards, the MABL grows steadily and reaching its peak at about 1400-1500 hrs and coming down thereafter. The deepening of the MABL is observed in the late afternoon during easterly monsoon period. Figure 9(b) shows the evolution of MABL in westerly monsoon period. On these days, a different scenario has been observed. A shallow MABL confined to about 1.1 km is observed on both the days. This is because during the westerly monsoon, boundary layer will be rich in moisture. So, most of the radiation will be utilized for the evaporation process, which results in a shallow MABL. One more cause for the shallow MABLs during the westerly monsoon days may be due to the increased upper level clouds that can reduce the incoming solar radiation. Similar features have been observed on most of the days in each category during the observational period.



**Fig. 9: Evolution of MABL on two (a) Easterly monsoon (b) Westerly monsoon days.**

To explain the shallow MABL heights during the westerly monsoon period, we investigated the effect of surface solar radiation and low level cold air advection on MABL height. Surface solar radiation plays an important role in driving the MABL, and variations due to clouds or aerosols can have a pronounced effect on MABL height. Fig. 10 shows the correlation between MABL height and surface solar radiation. Positive correlation exists between MABL height and surface solar radiation indicating that the MABL height increases with solar radiation.



**Fig. 10: Correlation between MABL height and surface solar radiation.**

Table 2 contains monthly means of solar radiation ( $\text{W m}^{-2}$ ) and the daily maxima solar radiation ( $\text{W m}^{-2}$ ). Overall, the large values of both solar radiation measures for the easterly monsoon period are indicative of mostly cloud-free conditions. The daily maximum MABL heights occur in April with values of approximately between 1.2 to 1.5 km, decreasing to 0.9 to 1.1 km in July. Due to large solar radiation during April, maximum MABL heights are observed.

Month	Jan	Feb	Mar	Apr	May	Jun	Jul	Aug	Sep	Oct	Nov	Dec
Mean SR	194.9	206.3	212.3	232.2	178	198.3	186.9	213.4	214	210.1	198.9	189.5
Max SR	832.9	814.7	804.3	860.2	684.6	745.7	743	797.2	814.1	845.4	796.6	710.5

**Table.2:** Monthly mean solar radiation (top number); and monthly mean hourly maximum solar radiation, SR (bottom number).

Cold-air advection within the boundary layer can help reduce MABL heights by counter-acting the warming due to surface heating from solar radiation. Figure 11 shows temperature advection for both the easterly and westerly monsoon periods. The advection is calculated as the temperature difference between monsoon period and the average temperature for the whole observational period, multiplied by the westerly wind component. Increased cold-air advection during the westerly monsoon period is evident, especially at lower levels and afternoon to evening hours. The strongest cold-air advection for these months begins in the early afternoon hours, after which the MABL decreases its height gradually. This cold-air advection is associated with the push of marine air into the inland region that occurs with the afternoon sea-breeze

circulation. Low-level cold-air advection will increase the stratification and will counteract the warming due to solar insolation, and will contribute to the shallower MABL heights during westerly monsoon period.

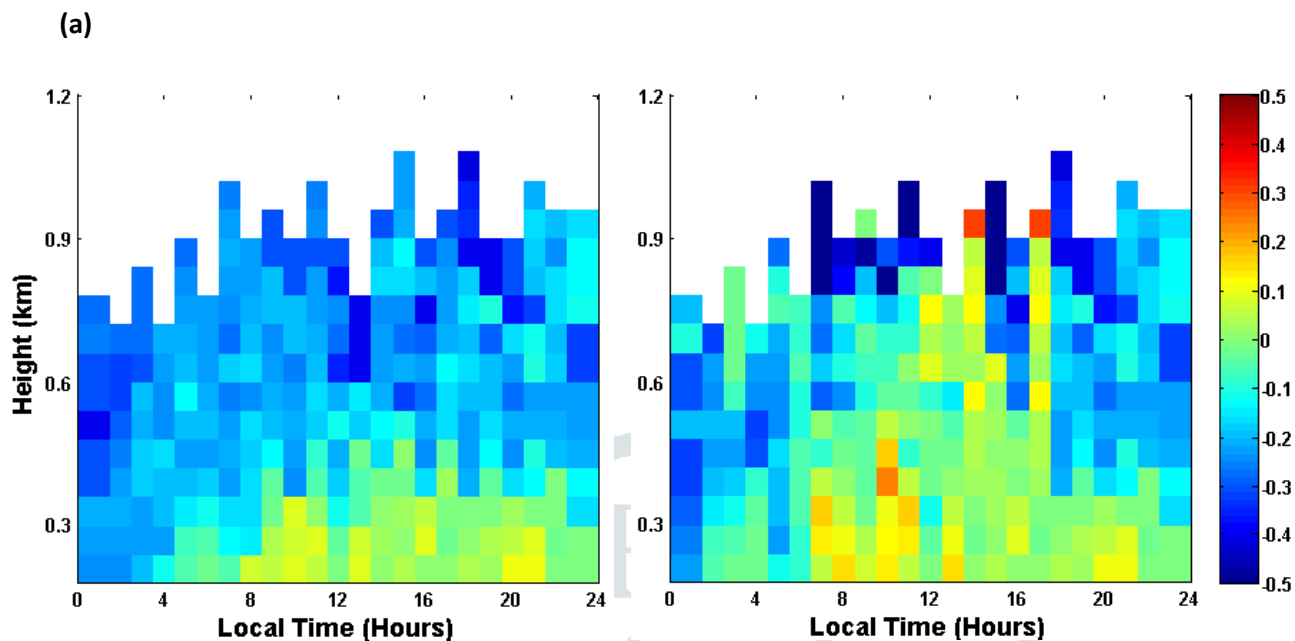


**Fig. 11:** Diurnal mean time–height cross section of virtual temperature advection for (a) Easterly (b) Westerly monsoon period.

## 5. Summary and Conclusions

The Wind profiler radar (WPR) is continuously operated since 09 March 2003. To check the WPR performance, a comparison study with Korrer radiosonde data is carried out. The results show fairly good agreement between the two measurements considering the spatial separation and data acquisition. The MABL height shows a diurnal variation with its maximum in the afternoon and decreases slowly reaching its minimum in the night. The seasonal variability of MABL height shows a maximum in the month of April and minimum in the month of September. The effect of surface solar radiation and low level cold air advection on MABL height is investigated. It is clear that, surface solar radiation is responsible for the maximum MABL height in the easterly monsoon period and cold air advection from the surrounding marine atmosphere is responsible for the shallow MABL heights during the westerly monsoon period.

## References

1. Liu, S., and X.-Z. Liang (2010) Observed diurnal cycle climatology of planetary boundary layer height, *J. Clim.(USA)*, **23**, 5790–5809.
2. Guo, P., Y.-H. Kuo, S. V. Sokolovskiy, and D. H. Lenschow (2011) Estimating atmospheric boundary layer depth using COSMIC radio occultation data, *J. Atmos. Sci.(USA)*, **68**, 1703–1713.
3. Ao, C. O., D. E. Waliser, S. K. Chan, J.-L. Li, B. Tian, F. Xie, and A. J. Mannucci, (2012) Planetary boundary layer heights from GPS radio occultation refractivity and humidity profiles, *J. Geophys. Res.(USA)*, **117**, D16117, doi:10.1029/2012JD017598.
4. McGrath-Spangler, E. L., and S. Denning (2012) Estimates of North American summertime planetary boundary layer depths derived from space-borne lidar, *J. Geophys. Res.(USA)*, doi:10.1029/2012JD017615.
5. Tucker, S. C., C. J. Senff, A. M. Weickmann, W. A. Brewer, R. M. Banta, S. P. Sandberg, D. C. Law, and R. M. Hardesty (2009) Doppler lidar estimation of mixing height using turbulence, shear, and aerosol profiles, *J. Atmos. Oceanic Technol.(USA)*, **26**, 673–688.
6. Lokoshchenko, M. A. (2002) Long-term sodar observations in Moscow and a new approach to potential mixing determination by radiosonde data, *J. Atmos. Oceanic Technol.(USA)*, **19**, 1151–1162.
7. Angevine, W. M., A. B. White, and S. K. Avery, (1994) Boundary layer depth and entrainment zone characterization with a boundary-layer profiler. *Boundary Layer Meteorology (NETHERLANDS)*, **68**, 375–385.
8. Bianco, L., and J. M. Wilczak, (2002) Convective boundary layer depth: improved measurement by doppler radar wind profiler using fuzzy logic methods. *J. Atmos. Oceanic Tech(USA)*, **19**, 1745-1758.
9. van der Kamp, D., and I. McKendry (2010) Diurnal and seasonal trends in convective mixed layer heights estimated from two years of continuous ceilometer observations in Vancouver BC, *Boundary Layer Meteorol.(NETHERLANDS)*, **137**, 459–475.
10. K.S.Gage, C.R.Williams, W.L.Clark, P.E. Johnston, and D.A.Carter, *J. Atmos.Ocean. Tech.(USA)*, **19**, 843 (2002).
11. Williams, C.R., W.L.Ecklund, and K.S.Gage, *J. Atmos.Ocean. Tech. (USA)*, **12**, 996 (1995).
12. K.K.Reddy, T. Kozu, Y.Ohno, K. Nakamura, A.Higuchi, K.Madhu Chandra Reddy, P.Srinivasulu, V.K.Anandan, A.R.Jain, P.B.Rao, R.RangaRao, G.Viswanthan, and D.N.Rao, *Radio Sci. (USA)*, **37**, 14-1 (2002).
13. K.K.Reddy, B. Geng, H.Yamada, H.Uyeda, R.Shirooka, T.Ushiyama, S.Iwasaki, H.Kubota, T.Chuda, K.Takeuchi, T.Kozu, Y.Ohno, K. Nakamura, D.N.Rao, *Monsoon precipitation characteristics over Asia and Western Tropical Pacific Ocean*, 6th International GAME Conference, Kyoto International Community House, Kyoto, Japan, 3-5 December 2004.